Translational Science

Cancer Research

RAS–MAPK Pathway-Driven Tumor Progression Is Associated with Loss of CIC and Other Genomic Aberrations in Neuroblastoma

Thomas F. Eleveld[1,2], Linda Schild[1], Jan Koster[2], Danny A. Zwijnenburg[2], Lindy K. Alles[1], Marli E. Ebus[1], Richard Volckmann[2], Godelieve A. Tijtgat[3], Peter van Sluis[2], Rogier Versteeg[2], and Jan J. Molenaar[1]

Abstract

Mutations affecting the RAS–MAPK pathway frequently occur in relapsed neuroblastoma tumors, which suggests that activation of this pathway is associated with a more aggressive phenotype. To explore this hypothesis, we generated several model systems to define a neuroblastoma RAS–MAPK pathway signature. Activation of this pathway in primary tumors indeed correlated with poor survival and was associated with known activating mutations in ALK and other RAS–MAPK pathway genes. Integrative analysis showed that mutations in PHOX2B, CIC, and DMD were also associated with an activated RAS–MAPK pathway. Mutation of PHOX2B and deletion of CIC in neuroblastoma cell lines induced activation of the RAS–MAPK pathway. This activation was independent of phosphorylated ERK in CIC knockout systems. Furthermore, deletion of CIC caused a significant increase in tumor growth *in vivo*. These results show that the RAS–MAPK pathway is involved in tumor progression and establish CIC as a powerful tumor suppressor that functions downstream of this pathway in neuroblastoma.

Significance: This work identifies CIC as a powerful tumor suppressor affecting the RAS-MAPK pathway in neuroblastoma and reinforces the importance of mutation-driven activation of this pathway in cancer. *Cancer Res; 78(21); 6297–307. ©2018 AACR.*

Introduction

Neuroblastoma is a pediatric tumor of the peripheral sympathetic nervous system, which has a highly variable clinical outcome (1). Whole genome sequencing (WGS) studies have identified recurrent aberrations primarily in *MYCN, ALK, ATRX,* and *TERT* (2–5). We recently identified that mutations that activate the RAS–MAPK signaling pathway occur frequently in neuroblastoma relapse tumors and that these mutations confer sensitivity to MEK inhibitors (6). As in other tumor types the RAS pathway is frequently affected in neuroblastoma through mutations in the RAS genes themselves, but also via mutations in regulatory proteins and downstream signaling components, like *NF1* and *PTPN11*, or constitutive activation of receptor kinases that trigger this pathway, like *ALK* (7). These results have led to the inclusion of neuroblastoma relapse patients in clinical trials with MEK inhibitors. However, the role of MEK inhibitors in an induction treatment protocol is under debate, since the role of active RAS–MAPK signaling in primary neuroblastoma tumors was not obvious.

Gene expression signatures of oncogenic pathways have been proven to be a powerful tool in cancer research. These signatures are able to identify patterns of pathway activation in cell lines and tumors and can also predict response to targeted therapeutics (8, 9). Several gene signatures for the RAS–MAPK pathway have been published and these show a wide range of genes being expressed downstream of RAS (8–10). Generally, expression of RAS–MAPK negative feedback regulators is associated with an active pathway, which suggests that it is very tightly regulated (9, 11). Moreover, the RAS–MAPK pathway affects expression of downstream transcription factors like the ETS family of transcription factors, c-FOS and MYC (12–14). One problem is that the majority of published signatures show little overlap (9), suggesting that the effects of RAS activation could be largely background dependent.

We developed a neuroblastoma RAS–MAPK gene signature to determine RAS–MAPK pathway activation in neuroblastoma primary tumors. Because WGS data of a lot of these tumors was available, the signature also enabled us to verify known mutational biomarkers for pathway activation and identify new biomarkers. We show that RAS–MAPK pathway activation is associated with poor prognosis in primary neuroblastoma tumors. Mutations in genes that are known to cause activation, such as *ALK, SOS1*, and *PTPN11*, are associated with high pathway activity. In other activated tumors, we detect recurrent aberrations in *CIC, DMD,* and *PHOX2B*. We show that these mutations affect this pathway to varying degrees both *in vitro* and *in vivo*. Especially deletion of *CIC* causes a significant increase in signature gene expression and growth speed *in vivo*. This increase is independent of phosphorylated ERK, indicating that *CIC* functions downstream of the RAS–MAPK pathway.

[1]Department of Translational Research, Princess Maxima Centre for Childhood Oncology, Utrecht, the Netherlands. [2]Department of Oncogenomics, Academic Medical Center of the University of Amsterdam, Amsterdam, the Netherlands. [3]Department of Pediatric Oncology, Emma Children's Hospital, Academic Medical Center of the University of Amsterdam, Amsterdam, the Netherlands.

Note: Supplementary data for this article are available at Cancer Research Online (http://cancerres.aacrjournals.org/).

Corresponding Author: Thomas F. Eleveld, Princess Maxima Center for Pediatric Oncology, Uppsalalaan 8, 3584CT Utrecht, the Netherlands. Phone: 003641044766; E-mail: t.f.eleveld@prinsesmaximacentrum.nl

doi: 10.1158/0008-5472.CAN-18-1045

Materials and Methods

Cell lines

All cell lines were cultured in DMEM supplemented with 10% FBS, 20 mmol/L L-glutamine, 10 U/mL penicillin, and 10 μg/mL streptomycin and maintained at 37°C under 5% CO_2. Cell line identities are confirmed by short tandem repeat (STR) profiling using the PowerPlex16 system and GeneMapper software (Promega) upon the start of culture. Cell lines are screened monthly for the presence of mycoplasma.

mRNA expression and WGS analysis

All analyses were performed using the R2 bio informatics platform (http://r2.amc.nl). Expression data of NRASQ61V overexpression, NF1 CRISPR lines, Trametinib and appropriate controls were profiled in triplicate on Affymetrix u133p2 arrays and are available under GSE115406. For our cohort of primary neuroblastoma tumors two expression series (GSE16476 and GSE73537) were combined, and batch correction with the combat algorithm in R was applied to control for the different labeling kits used. Accession numbers of other used datasets can be found in Supplementary Table S1.

Heatmaps represent *z*-score normalized data and is represented in the order of clustering. Colored boxes (tracks) above or below expression data represent sample characteristics or clustering outcome. Signature scores were calculated as the average *z*-score of the signature genes.

For mutational analyses WGS data of 88 primary neuroblastoma tumors (EGA, EGAS00001000222) combined with 21 additional tumors (EGA, EGAS00001001479) was analyzed as was published before.

Lentiviral packaging and transfection

Lentivirus was packaged by cotransfection of constructs with the third-generation packaging plasmids pMD2.G, pRRE, and pRSV/REV with Fugene HD (Roche) into HEK293T cells. Cell lines were lentivirally infected and subsequently selected with blasticidin or puromycin.

Generation of CRISPR and overexpression lines

Cells were transduced with virus produced from pLenti-CRISPRv2 (15) with the appropriate gRNA sequences (Supplementary Table S2) or pInducer (6) with open reading frames for the mentioned protein and selected with puromycin. Genomic DNA was isolated and CRISPR efficiency verified using PCR and subsequent Sanger sequencing. pLentiCRISPR v2 was a gift from Feng Zhang (Addgene plasmid #52961).

Western blot analysis

Samples of inducible overexpression lines were harvested after 72 hours exposure to doxycycline. Samples were lysed in Laemli buffer and subjected to Western blotting with antibodies against RAS (Cell Signaling Technology; #3965), total ERK (Cell Signaling Technology; #9102), pMEK (Cell Signaling Technology; #9154), pERK (Cell Signaling Technology; #9101), total MEK (Cell Signaling Technology; #8727), NF1 (Santa Cruz Biotechnology sc-67), and PHOX2B (Santa Cruz Biotechnology sc-376997).

qRT-PCR

RNA was isolated using Trizol and purified using RNAeasy columns (Qiagen). cDNA was generated from 2.5 μg of RNA using the IScript cDNA Synthesis Kit (Bio-Rad) according to the manufacturers protocol. Gene expression was determined using SYBR green (Bio-Rad) on a C1000 thermal cycler (Bio-Rad). *HPRT1*, *SDHA*, and *UBC* were used as reference genes to normalize gene expression. Primer sequences can be found in Supplementary Table S3.

Xenograft experiments

All experiments were conducted after obtaining ethical approval from the DEC (animal experiments committee) of the AMC under number DAG103101. NMB cell lines were generated as described above and 2×10^6 cells were xenografted into female NMRI nu-/nu- mice at 5 to 7 weeks of age ($n = 6$ per group). Tumor size was monitored two times a week. Tumor burden was determined according to the formula $(\pi/6)d^3$, where d represents the mean tumor diameter obtained by caliper measurement. Mice were sacrificed when tumors volumes exceeded 1,000 mm^3. Statistical analysis was performed using a Gehan Breslow Wilcoxon test to determine significant differences between survival curves.

Results

A six gene core signature marks the RAS–MAPK activation state of neuroblastoma cells

To identify transcriptional changes associated with activation of the RAS–MAPK signaling pathway in neuroblastoma, we generated several cell line systems in which this pathway is activated. Activating mutations in *NRAS* and inactivation of *NF1* are both associated with increased RAS–MAPK signaling and occur at low frequency in neuroblastoma tumors (7, 16). An NRASQ61V mutated protein was overexpressed and the *NF1* gene was inactivated using CRISPR, both in the cell line NMB. This cell line did not contain any known mutations affecting the RAS–MAPK pathway on forehand as determined by WGS and did not show activation of RAS–MAPK signaling pathway (Supplementary Fig. S1). Both overexpression of mutated *NRAS* and inactivation of *NF1* caused activation of the RAS–MAPK signaling pathway as measured by Western blot analysis (Fig. 1A). Gene expression profiling was performed for all cell lines and appropriate controls.

Mutations in *NRAS* and *NF1* are also known to activate other signaling pathways. To further restrict the gene set to only genes directly associated with RAS–MAPK signaling, we performed gene expression profiling of the cell line SJNB8 treated with the MEK inhibitor Trametinib for 6 hours. SJNB8 has a *KRAS G12D* mutation and concordantly shows high levels of phosphorylated ERK on Western blot analysis, which is completely abrogated by treatment with 1 μmol/L Trametinib for 6 hours (Fig. 1B).

Genes that were regulated by expressing the different mutations and were conversely regulated by MEK inhibitor treatment by more than 2.5-fold were included in the mRNA signature (Supplementary Table S4; Supplementary Fig. S2). Gene set enrichment analysis of the differentially expressed genes shows KRAS signaling as the top enriched category for each treatment (Supplementary Table S5), suggesting that changes in RAS–MAPK pathway were indeed the most relevant change in our models. Analysis of the overlapping genes yields a set of six genes that are consistently upregulated upon activation and downregulated upon inhibition of the RAS–MAPK pathway (Fig. 1C). This set contains several genes that are known to be associated with

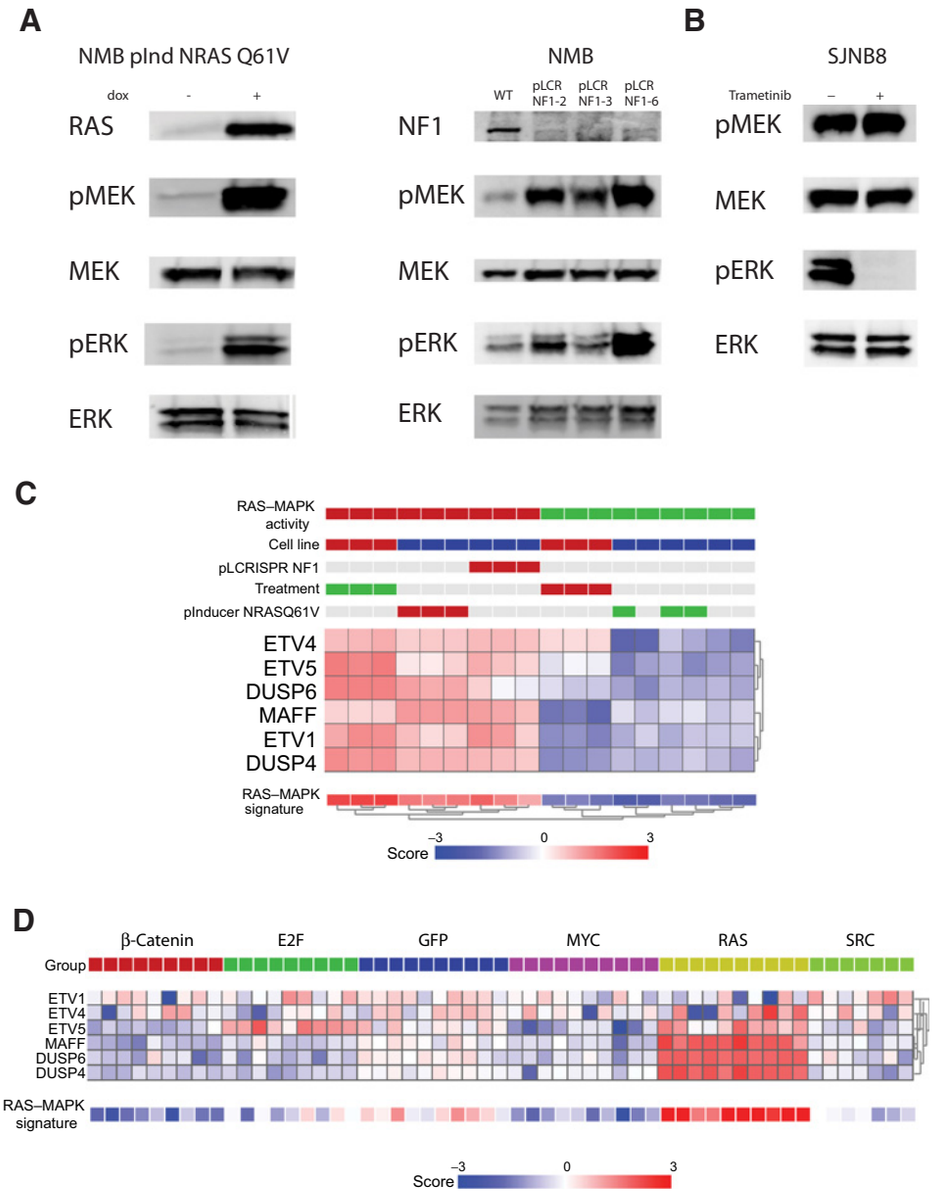

Figure 1.
Deriving a neuroblastoma RAS–MAPK gene expression signature. **A,** Western blot analysis shows RAS–MAPK pathway activation after overexpression of mutated *NRAS* and *NF1* knockout in the neuroblastoma cell line NMB. **B,** Western blot analysis of the cell line SJNB8 treated with 1 μmol/L Trametinib for 6 hours shows inactivation of the RAS–MAPK pathway. **C,** Genes included in the signature are highly expressed in conditions where the pathway is active (red track) and lowly expressed when the pathway is inactive (green track). **D,** Expression of RAS–MAPK signature genes is high in keratinocytes where constitutively active RAS is expressed (yellow track), as determined by microarray analysis. In controls and lines transfected with other oncogenes (other colors), expression of these genes is low.

RAS–MAPK signaling in other systems and are part of established RAS–MAPK signatures, such as *DUSP4*, *DUSP6*, and *ETV4* (9, 17). Analysis of expression data from keratinocytes transfected with different oncogenes shows a strong upregulation of these six genes in RAS transfected cells in contrast to cells transfected with GFP or other oncogenes, showing that upregulation of these genes is specifically associated with increased RAS signaling in multiple cell systems (Fig. 1D; ref. 8).

High signature scores are associated with mutation status and sensitivity to MEK inhibition in neuroblastoma cell lines

To assess the use of this gene signature in neuroblastoma, we used our panel containing 17 neuroblastoma cell lines. Twelve of these cell lines contain mutations affecting RAS–MAPK signaling (*ALK*, *NF1*, *RAS*, and *BRAF*) and it was previously shown that mutation status is associated with sensitivity to MEK inhibition in these cell lines (6). We confirmed that mutation status also correlates with phosphorylated MEK and ERK on Western blot analysis (Supplementary Fig. S1).

Expression data from this cell line panel was subjected to k-means clustering in two groups using the signature genes. The cell lines with mutations affecting the RAS–MAPK pathway cluster together on one side and consistently show high expression of the signature genes (Fig. 2A). Furthermore, when the average expression of these genes is calculated as one signature score per cell line, these signature scores show significant differences between mutated and nonmutated cell lines (Supplementary Fig. S3). Signature scores also correlate with MEK and ERK phosphorylation and sensitivity to three different MEK inhibitors (Fig. 2B and C).

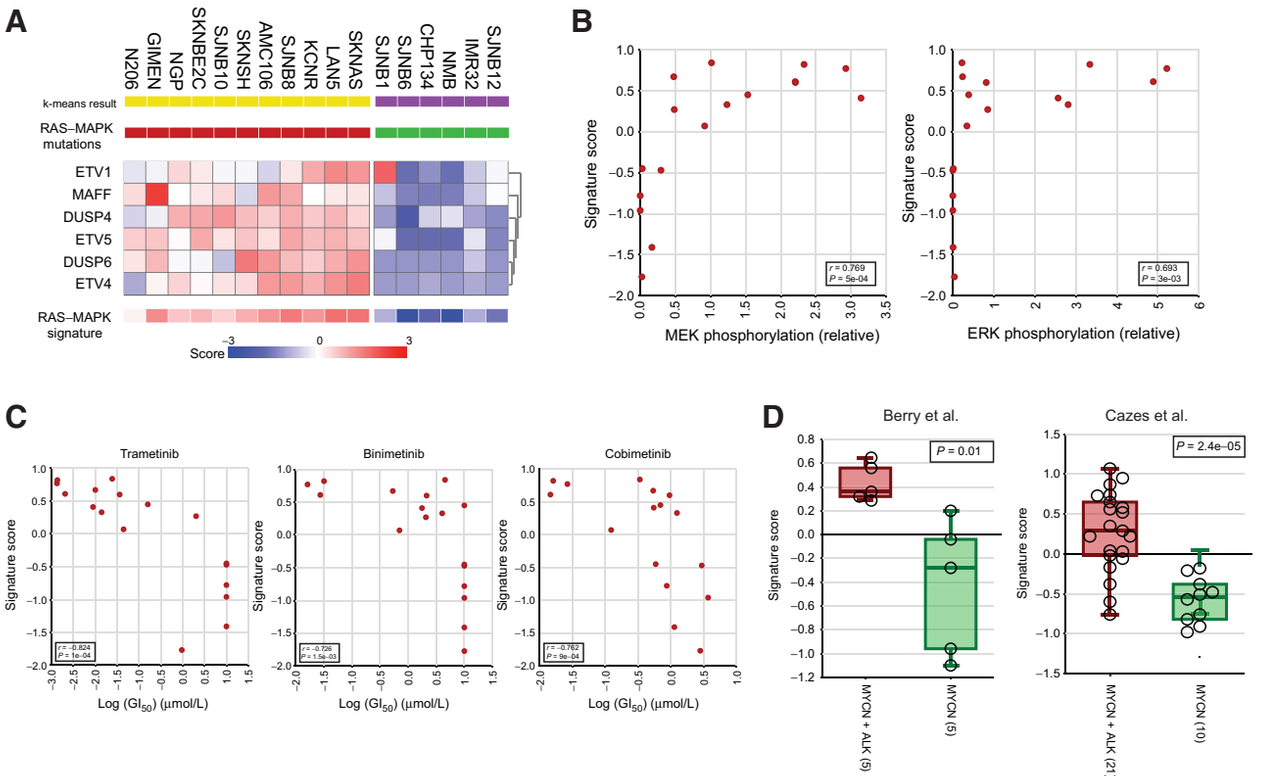

Figure 2.

Signature expression correlates with phenotypic markers of pathway activation in neuroblastoma models *in vitro* and *in vivo*. **A,** k-means clustering of microarray expression data of a panel of neuroblastoma cell lines. Tracks represent the k-means result (purple and yellow) and mutation status (red, mutations affecting RAS–MAPK; green, no mutations). This clustering result was identified in 25/25 k-means iterations. **B,** Correlation between signature score and relative MEK and ERK phosphorylation as determined by Western blot analysis. *P*- and *R*-values were determined by Spearman rank correlation and are shown in the lower right corner. **C,** Correlation between signature scores and sensitivity to different MEK inhibitors. *P*- and *R*-values were determined by Spearman rank correlation and are shown in the lower right corner. **D,** Signature scores in neuroblastoma tumors from transgenic mouse models from either MYCN amplification or MYCN amplification combined with ALK mutations. *P*-values were generated using a two-sided Students *t* test.

The same analyses were performed in an independent dataset containing 23 neuroblastoma cell lines for which mutation status and sensitivity to a variety of targeted inhibitors is available (18). Again, all mutated cell lines show high signature scores. One cell line for which no mutations were reported also clustered together with the positive lines, suggesting that this line may contain undetected mutations that activate this pathway (Supplementary Fig. S4A). Also in this dataset signature scores correlate with sensitivity to three different MEK inhibitors, which are distinct from the ones in the previous analysis (Supplementary Fig. S4B). These results suggest that the RAS–MAPK gene signature can accurately determine the activation of this pathway and sensitivity to targeted treatment in neuroblastoma cell lines.

Transgenic neuroblastoma models containing ALK mutations show high signature scores

To determine if this signature also performs well *in vivo*, analyses were performed in mRNA profiles of transgenic neuroblastoma mouse models. In transgenic mice, *MYCN* amplification alone is enough to induce tumor formation; however, tumors that also contain *ALK* mutations display increased RAS–MAPK signaling and have a shorter latency and are much more aggressive (19, 20). The tumors that have both *ALK* mutations and *MYCN* amplification have significantly higher signature scores than the tumors with only *MYCN* amplification in both datasets (Fig. 2D), consistent with the observation that *ALK* mutations activate RAS–MAPK signaling in these models. This shows that expression of our signature also correlates with activation of this pathway *in vivo* in neuroblastoma mouse models.

High expression of the RAS–MAPK signature genes is associated with poor prognosis in primary tumors

The RAS–MAPK gene signature was used in expression data of our set of 122 primary neuroblastoma tumors to determine the effect of pathway activation on prognosis. The data were subjected to k-means clustering in two groups, which divides the tumors into a group of 26 tumors with high expression of the signature genes and a group of 96 tumors with low expression (Fig. 3A; Supplementary Fig. S5A). The patient group represented in the cluster with high expression showed a significantly shorter overall survival than the patients in the cluster with low expression (Fig. 3B; Supplementary Fig. S5B). The same analysis was performed in an independent larger dataset of primary neuroblastoma containing 498 tumors (21). Also here, a smaller group (126/498) of tumors clustered together and showed high expression of the gene signature and this was associated with

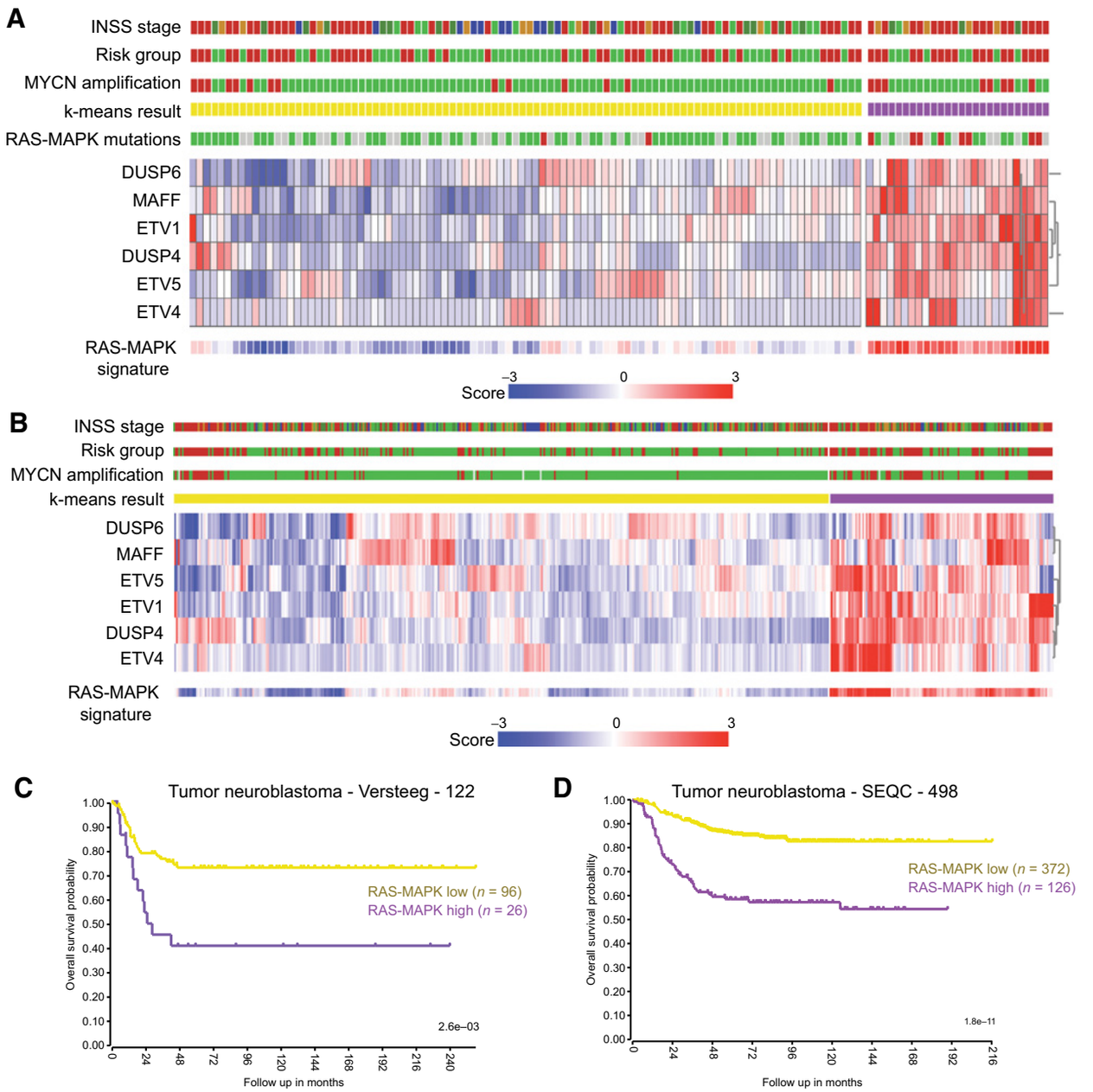

Figure 3.

Activation of the RAS–MAPK pathway as determined by the gene expression signature is associated with poor prognosis in primary neuroblastoma tumors. **A,** k-means clustering of expression data of a cohort of 122 primary neuroblastoma tumors. Tracks represent the k-means result (purple and yellow), INSS stage (light green, stage 1; dark green, stage 2; yellow, stage 3; red, stage 4; blue, stage 4S), risk group (red, high risk; green, low risk), and MYCN amplification status (red, MYCN amplified; green, non-MYCN amplified). This clustering result was identified in 25/25 k-means iterations. **B,** k-means clustering of expression data of set of 498 primary neuroblastoma tumors. Tracks represent the k-means result (purple and yellow), INSS stage (light green, stage 1; dark green, stage 2; yellow, stage 3; red, stage 4; blue, stage 4S), risk group (red, high risk; green, low risk), and MYCN amplification status (red, MYCN amplified; green, non-MYCN amplified). k-means clustering was performed 10 times and the most prevalent result was chosen. This clustering result was identified in 14/25 k-means iterations. Kaplan–Meier curve of the overall survival based on the clustering performed in **A**. *P* values were generated through log-rank test. **C,** Kaplan–Meier curve of the overall survival based on the clustering performed in **A**. *P* values were generated through log-rank test. **D,** Kaplan–Meier curve of the overall survival based on the clustering performed in **B**. *P* values were generated through log-rank test.

significantly shorter overall survival (Fig. 3C and D). In both datasets, pathway activation was also associated with shorter progression-free survival (Supplementary Fig. S6A and S6B). These results suggest that the RAS–MAPK pathway is more active in a subset of neuroblastoma tumors and that activation of this pathway is associated with poor prognosis.

Neuroblastoma is classified in five stages (1–4S) with stage 4 being the most aggressive. To determine if the prognostic effect of activation of RAS–MAPK signaling is caused by association with a higher stage we looked at the effect of RAS–MAPK activation on survival within each stage. Multivariate cox proportional hazard analysis shows that RAS–MAPK activation is still a significant predictor for survival when we take risk group into account (Supplementary Table S6). Accordingly, pathway activation is associated with worse prognosis in stage 3 and 4 tumors (Supplementary Fig. S7A and S7B), showing that the effect of RAS–MAPK pathway activation on survival is not caused solely by association with a specific stage. In stage 1 and 2 and 4S, there is no clear correlation between RAS–MAPK pathway activation and survival (Supplementary Fig. S7C–S7E). These results suggest that RAS–MAPK activation does not determine tumor stage but does cause a more aggressive tumor when it occurs in high stages.

We also observe that pathway activation as determined by clustering is associated with MYCN amplification in the larger dataset (Fisher exact *P* value = 6.03e−16), suggesting that the two events may cooperate. However, in a set of only non-MYCN amplified tumors the patients with tumors that cluster in the group with high expression still have a significantly poorer prognosis (Supplementary Fig. S8A and S8B; ref. 22). Moreover, Cox proportional hazards analysis show a significant association with survival also if we take MYCN amplification into account in the larger dataset, whereas this is borderline significant in our dataset (Supplementary Table S6). These data suggest that the effect of RAS–MAPK pathway activation on prognosis is not dependent on MYCN amplification. Activation of telomere maintenance through mutations in TERT and ATRX was also recently shown to be an important risk factor for poor prognosis, however, these groups were too small to test the association between an activated RAS–MAPK pathway and the presence of these mutations (Supplementary Fig. S8C).

The presence of RAS–MAPK mutations in tumors is associated with higher signature scores

To determine if activation of this pathway is associated with the presence of activating mutations, we analyzed WGS data (available for 67 of 122 tumors) and targeted sequencing data for *PHOX2B* and *ALK* of these tumors. We detect mutations that have been described to activate the RAS–MAPK pathway in 10 tumors (Supplementary Table S7), and eight of these fall into the MEK active cluster (Fisher exact *P*-value = 3.4E−07). These are mostly mutations in *ALK*, but also mutations in other genes associated with RAS–MAPK signaling such as *PTPN11*, *SOS1*, and *NF1*. Tumors with these mutations have significantly higher signature scores than tumors without (Supplementary Fig. S9).

To identify potential other genetic aberrations that lead to activation of this signaling pathway in neuroblastoma, genes were selected that were mutated two times or more in the RAS–MAPK active cluster (Fig. 4A). We previously identified several tumors with frameshift or nonsense mutations in *PHOX2B* (23), of which five were also present in this dataset (Fig. 4B). Three of these tumors fall into the RAS-MAPK active group as determined by k-means clustering, whereas the other two also show relatively high signature scores. Furthermore, two tumors in the RAS-MAPK active cluster show deletions in the *DMD* gene (Fig. 4C) and two other tumors from this cluster show homozygous inactivation of the *CIC* locus (Fig. 4D). In our series of 108 tumors that were subjected to WGS a third tumor with homozygous inactivation of *CIC* was detected (Supplementary Fig. S10). Unfortunately, no mRNA expression data was available for this tumor.

To determine if these aberrations play a role in the activation of the RAS–MAPK pathway in neuroblastoma, we generated overexpression or knockout cell lines. Because *PHOX2B* mutations are thought to exert a dominant negative effect (24), a mutant PHOX2B protein derived from the SKNSH cell line was expressed in the NMB and SJNB1 cell lines (Fig. 4B). This indeed leads to activation of this signaling pathway as identified by Western blot analysis, whereas this activation was not observed when wild-type *PHOX2B* was expressed (Fig. 5A).

Inactivation of *CIC* in similar locations as the breakpoints detected in the tumors using CRISPR-CAS9 did not lead to an increase in MEK and ERK phosphorylation (data not shown). It did, however, lead to upregulation of the signature genes compared with the unmodified cell line (Fig. 5B). CIC is known to function downstream of ERK and is involved in the activation of ERK target genes (25). Indeed, treating the *CIC* mutant NMB line with Trametinib does not cause a shift of the *CIC* mutated line from the active to the inactive cluster, indicating that expression of the signature genes is not severely affected. In contrast, this shift is induced by treating *NF1* deleted lines with Trametinib (Fig. 5B). These suggest that loss of *CIC* induces expression of RAS–MAPK target genes independent of activated ERK. In lines where *DMD* was knocked out or where mutant *PHOX2B* was overexpressed, no increased expression of the signature genes was observed (Supplementary Fig. S11).

Mutations in NRAS and CIC activate the RAS–MAPK pathway and activation increases neuroblastoma tumorigenicity

To test the hypothesis that activation of RAS–MAPK signaling leads to increased tumorigenicity in neuroblastoma, the NMB lines modeling the various mutations were used in xenograft experiments. Doxycycline induced expression of NRAS Q61V in xenograft tumors causes activation of the RAS–MAPK pathway as measured by increased expression of RAS–MAPK signature genes, although the difference is not as clear as *in vitro* (Fig. 5C). This was associated with increased tumor growth and a significantly shorter survival time than mice engrafted with the same cells that did not receive doxycycline (Fig. 5D). We did not observe effects on tumor growth induced by expression of mutant *PHOX2B* or knockout of *DMD* using CRISPR. Concordantly, no increased expression of the RAS–MAPK signature genes was observed (Supplementary Fig. S12A and S12B).

Inactivation of *CIC* in our xenograft tumors does cause a significant increase in the expression of RAS–MAPK signature genes (Fig. 5C) and a significantly shorter survival (Fig. 5D). We observed *in vitro* that deletion of *CIC* caused increased expression of the signature genes without inducing ERK phosphorylation. The observation that *CIC* deletions cause increased tumor growth suggests that expression of the RAS–MAPK target genes induces the functional effects of an activated RAS–MAPK pathway, even in the absence of active ERK. This also suggests that tumors with *CIC* inactivation will not respond to MEK inhibition, because the pathway is activated downstream of the target of the inhibitor. In

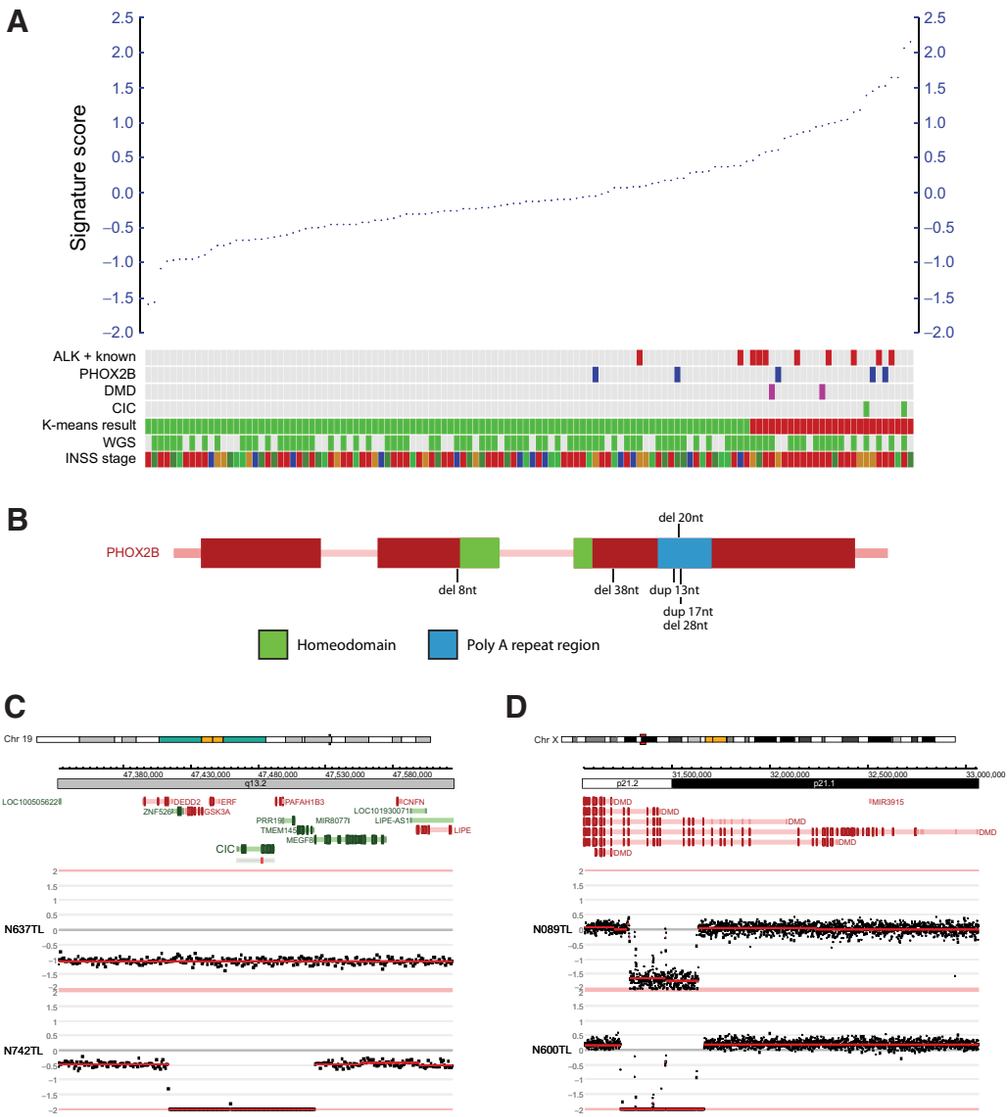

Figure 4.

High signature scores occur in tumors with mutations known to be associated with RAS–MAPK signaling and novel candidates. **A,** Signature scores for all 122 tumors. Tracks represent the presence of mutations, the k-means clustering result from Fig. 3A, whether the tumors were profiled using WGS and the INSS stage (light green, stage 1; dark green, stage 2; yellow, stage 3; red, stage 4; blue, stage 4S). **B,** Schematic overview of the *PHOX2B* locus. Introns, light red; exons, dark red. Bars below the structure represent the mutations found in the tumors (del, deletion; dup, duplication). The bar above the structure represents the mutation from the cell line SKNSH that was cloned and used for functional analyses. **C,** Coverage based copy number plots of the genomic situation in the *CIC* locus of the two tumors that show homozygous inactivation. Tumor 742 shows a homozygous deletion of the complete coding region, whereas tumor 637 shows a heterozygous deletion combined with a nonsense mutation at the location indicated by the red box. **D,** Coverage-based copy number plots of the genomic situation in the *DMD* locus of the two tumors that show inactivation. Both tumors show a deletion that leaves the smallest isoform intact and disrupts the larger isoforms.

line with this hypothesis, the presence of inactivating mutations in *CIC* were identified as the strongest predictor of resistance to Trametinib in a pan-cancer panel of 930 cell lines (Supplementary Fig. S13; ref. 26; https://www.cancerrxgene.org).

Discussion

In this paper we show through a mRNA signature that increased RAS–MAPK pathway activity in primary neuroblastoma tumors is associated with a poor prognosis. In several tumors with an active signature, previously described mutations are present that can account for activation of this pathway. Furthermore, we show that activation of this pathway *in vivo* promotes tumor growth. Finally, we identify *CIC* as a tumor suppressor in neuroblastoma that induces the downstream effects of RAS–MAPK pathway activation, whereas not directly affecting activation of the pathway itself (Fig. 6).

The mRNA signature was generated through analysis of gene expression data of activation and inhibition of the RAS–MAPK pathway in neuroblastoma cell lines. The stringent analysis yields

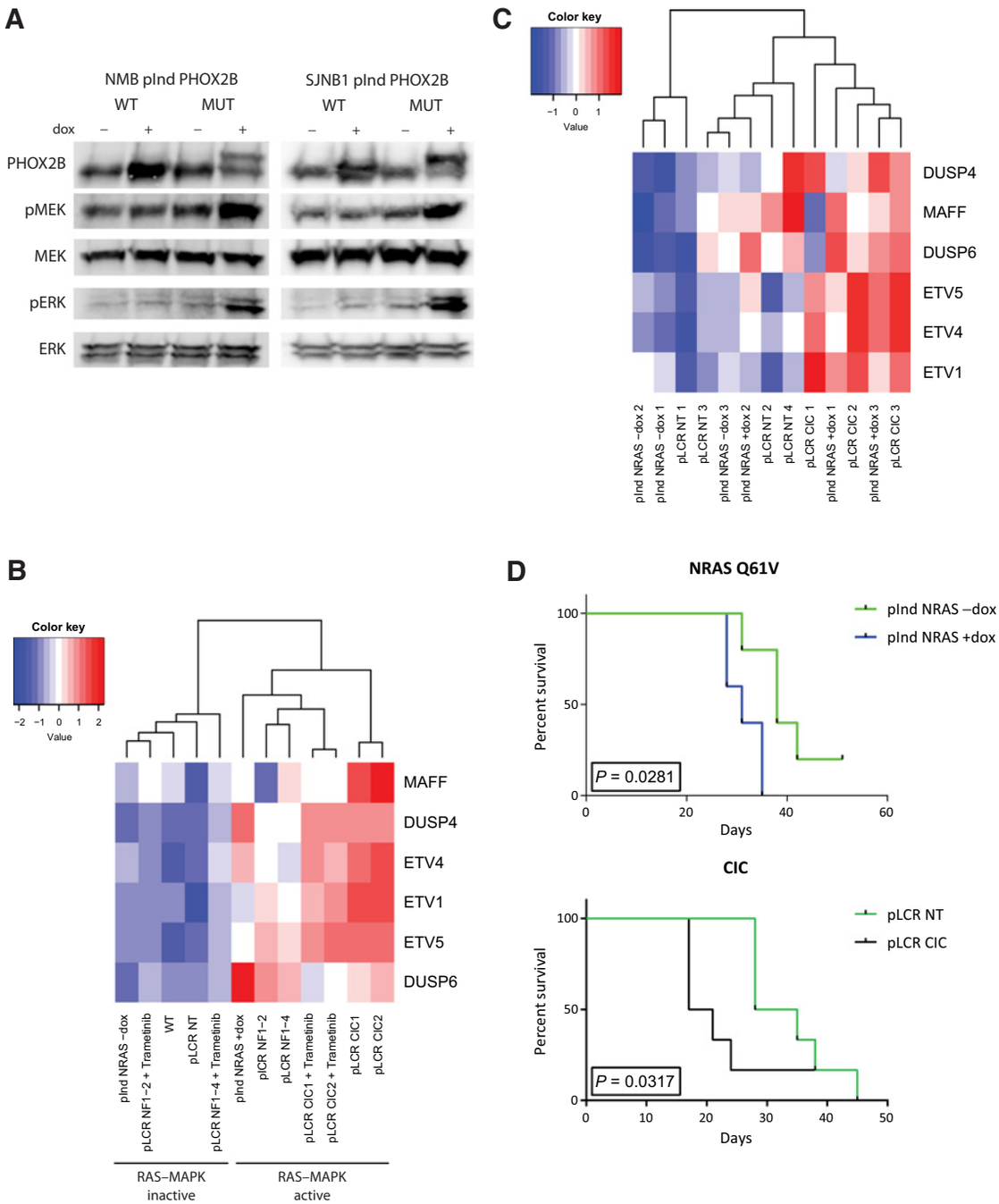

Figure 5.
Mutations in *PHOX2B* and *CIC* induce RAS–MAPK activation in neuroblastoma cell lines. **A,** Western blot analysis of the neuroblastoma cell lines NMB and SJNB1 expressing wild-type and mutant PHOX2B proteins shows activation of the RAS–MAPK pathway only by expression of mutant PHOX2B. **B,** Heatmaps representing gene expression of signature genes in the cell line NMB and modified daughter lines as determined by RT-qPCR. **C,** Heatmaps representing gene expression of signature genes in xenografts of the cell line NMB and modified daughter lines as determined by RT-qPCR. **D,** Kaplan–Meier curves of xenografts of NMB lines with inducible overexpression of NRAS Q61V with and without doxycycline and NMB with *CIC* knockout and nontargeting CRISPR constructs. *P* values were generated using the Gehan–Breslow–Wilcoxon test.

a list of only six genes, but the expression of these genes is highly correlated with MEK and ERK phosphorylation and sensitivity to MEK inhibition in cell lines, suggesting it has functional relevance. Furthermore, the observation that several of these genes, like *DUSP4* and *DUSP6*, are bona fide RAS–MAPK target genes strengthens this hypothesis (9, 17).

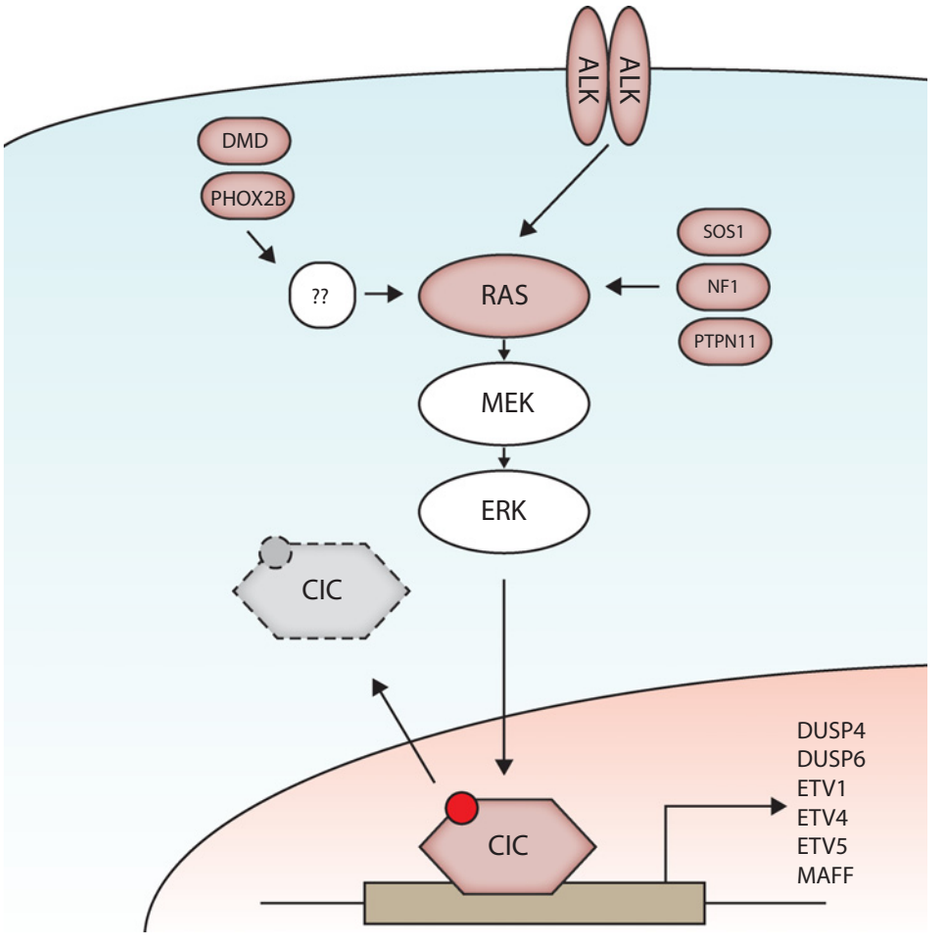

Figure 6.
Mutation driven RAS–MAPK activation in neuroblastoma. Diagram showing the mutated genes and their (hypothesized) role in RAS–MAPK activation in neuroblastoma.

When used in tumor series, the gene signature identifies a group of tumors that have high activation of the pathway and a significantly worse prognosis. However, activation of the pathway is only weakly associated with higher stage and happens across all stages, reminiscent of *ALK* mutations, which show a similar distribution and relationship to prognosis (27). This suggests that RAS–MAPK activation can occur in all tumor stages, and is not necessarily associated with a high-risk phenotype. When it occurs in high-risk tumors, however, it is associated with a significantly poorer prognosis. Whether activation of this pathway is also associated with poor prognosis in low risk tumors, remains to be determined, because it is possible that our study was underpowered to detect this effect.

We also observe an association between pathway activation and MYCN amplification, suggesting that these events may cooperate. It is known that activated RAS can stabilize the MYCN protein in neuroblastoma (28), which could explain our observations. However, high expression of the signature is still associated with poor prognosis in non-MYCN amplified tumors, showing that its effect is not only dependent on MYCN amplification.

Gene signatures provide valuable insight into the biology behind cancer. However, classification based on these signatures is highly dependent on the context of the patient cohort used and can, therefore, be difficult to reproduce, so their use as biomarkers for treatment is limited (29). Mutations are generally easier to detect and may provide a more robust biomarker of pathway activation and the application of targeted treatment. Therefore, we combined the mRNA signatures with mutational data and identify that mutations in certain genes are associated with activation of the RAS–MAPK pathway in neuroblastoma.

Mutations in genes known to activate the pathway were identified in 8/26 tumors, which were classified as RAS–MAPK active by clustering. This means that 31% of active tumors show possible causative mutations for RAS–MAPK pathway activity. Not all tumors were profiled using WGS, so it is possible that this frequency is even higher. These suggest that it is feasible to detect RAS–MAPK active tumors, which may be amenable to MEK inhibitor treatment, using mutations as a biomarker. Similar analyses in larger datasets of matched expression and mutation data will hopefully yield more biomarkers to also detect the remainder of active tumors. This would obviate the need for clinical use of our gene signature and the associated downsides.

We observed high signature scores in tumors with mutations in *PHOX2B* and *DMD*. However, mimicking these mutations did not cause activation of the signature genes nor an increase in tumor growth, although some activation of the pathway could be shown on Western blot analysis for *PHOX2B*. However, overexpression of *NRAS Q61V*, a strong oncogenic driver of RAS–MAPK signaling, only caused a modest increase in tumor growth. Therefore, it is possible that our study was underpowered to detect the effect of

other mutations. Moreover, the unmodified NMB xenograft line already showed very rapid growth. This could indicate that it has acquired other aberrations that have a similar functional effect as RAS–MAPK pathway activation, complicating the detection of effects induced by our treatment.

Mutations in *PHOX2B* were previously linked to retinoic acid resistance in neuroblastoma (30), which was also reported for RAS–MAPK activation through *NF1* deletion (16). Losses in *DMD* were recently reported as oncogenic drivers in tumors from the myogenic lineage (31), whereas mouse models where *DMD* is deleted show a high frequency of embryonal rhabdomyosarcoma (32), a myogenic tumor that is frequently driven by RAS hyper-activation. These indirect links between these mutations and RAS–MAPK activation merit further study of these genes in neuroblastoma.

We did observe strong activation of our signature genes by deletion of *CIC* and a significant increase in tumor growth. Inactivation of the *CIC* gene was recently described to drive metastasis in various cancer types (33). The Capicua tumor suppressor normally represses transcriptional changes induced by activated ERK by binding to promoter region of these genes (34). Active ERK causes detachment of CIC from the DNA, thereby enabling transcription of these genes. Loss of CIC therefore induces downstream gene expression independent of ERK. In concordance with this, we see induction of signature gene expression in *CIC* knockout lines, which cannot be inhibited by MEK inhibitor treatment. This means that MEK inhibitor treatment is not expected to be effective in *CIC* mutated tumors, which is concordant with *CIC* mutations being the strongest predictor for resistance to the MEK inhibitor Trametinib (https://www.cancerrxgene.org; ref. 26). Homozygous inactivation of *CIC* was detected in 3 of 108 of tumors in our series (5, 35). Another study detected focal deletions in *CIC* in 3 of 30 high-stage neuroblastoma tumors; ref. 36). These suggest that loss of *CIC* occurs relatively frequently in neuroblastoma and that further research is necessary to identify appropriate therapeutic targets for tumors with these aberrations.

Recent targeted and WGS studies have shown that mutations in known RAS–MAPK genes, such as *NF1*, *NRAS*, and *PTPN11*, occur in primary neuroblastoma tumors (7, 16). Although the relative frequency of each mutation is low, the cumulative incidence of these known mutations combined with the putative new aberrations we identify represents a significant part of the aggressive primary neuroblastoma tumors. For tumors with *ALK* mutations, an *ALK* inhibitor may be a more suitable treatment, but for tumors with other mutations MEK inhibitors may be a viable therapeutic strategy. Further research should therefore indicate whether the presence of these mutations in neuroblastoma tumors can indeed be used as a biomarker for treatment with MEK inhibitors.

Disclosure of Potential Conflicts of Interest

No potential conflicts of interest were disclosed.

Authors' Contributions

Conception and design: T.F. Eleveld, J.J. Molenaar
Development of methodology: T.F. Eleveld, L. Schild, J.J. Molenaar
Acquisition of data (provided animals, acquired and managed patients, provided facilities, etc.): T.F. Eleveld, L. Schild, G.A. Tijtgat, R. Versteeg
Analysis and interpretation of data (e.g., statistical analysis, biostatistics, computational analysis): T.F. Eleveld, J. Koster, D.A. Zwijnenburg, R. Volckmann, J.J. Molenaar
Writing, review, and/or revision of the manuscript: T.F. Eleveld, L. Schild, L.K. Alles, G.A. Tijtgat, J.J. Molenaar
Administrative, technical, or material support (i.e., reporting or organizing data, constructing databases): L. Schild, J. Koster, D.A. Zwijnenburg, L.K. Alles, M.E. Ebus, R. Volckmann, P. van Sluis, R. Versteeg,
Study supervision: T.F. Eleveld, J.J. Molenaar

Acknowledgments

The research in this paper was supported by the Kinder Kankervrij Foundation (KiKa) under grants nos. 132 and 189 (primary recipient: Jan J. Molenaar).

The costs of publication of this article were defrayed in part by the payment of page charges. This article must therefore be hereby marked *advertisement* in accordance with 18 U.S.C. Section 1734 solely to indicate this fact.

Received April 11, 2018; revised June 21, 2018; accepted August 7, 2018; published first August 16, 2018.

References

1. Maris JM. Recent advances in neuroblastoma. N Engl J Med 2010;362:2202–11.
2. Chen Y, Takita J, Choi YL, Kato M, Ohira M, Sanada M, et al. Oncogenic mutations of ALK kinase in neuroblastoma. Nature 2008;455:971–4.
3. Cheung N-KV, Zhang J, Lu C, Parker M, Bahrami A, Tickoo SK, et al. Association of age at diagnosis and genetic mutations in patients with neuroblastoma. JAMA 2012;307:1062–71.
4. Seeger RC, Brodeur GM, Sather H, Dalton A, Siegel SE, Wong KY, et al. Association of multiple copies of the N-myc oncogene with rapid progression of neuroblastomas. N Engl J Med 1985;313:1111–6.
5. Valentijn LJ, Koster J, Zwijnenburg DA, Hasselt NE, van Sluis P, Volckmann R, et al. TERT rearrangements are frequent in neuroblastoma and identify aggressive tumors. Nat Genet 2015;47:1411–4.
6. Eleveld TF, Oldridge DA, Bernard V, Koster J, Daage LC, Diskin SJ, et al. Relapsed neuroblastomas show frequent RAS-MAPK pathway mutations. Nat Genet 2015;47:864–71.
7. Pugh TJ, Morozova O, Attiyeh EF, Asgharzadeh S, Wei JS, Auclair D, et al. The genetic landscape of high-risk neuroblastoma. Nat Genet 2013;45:279–84.
8. Bild AH, Yao G, Chang JT, Wang Q, Potti A, Chasse D, et al. Oncogenic pathway signatures in human cancers as a guide to targeted therapies. Nature 2006;439:353–7.
9. Dry JR, Pavey S, Pratilas CA, Harbron C, Runswick S, Hodgson D, et al. Transcriptional pathway signatures predict MEK addiction and response to selumetinib (AZD6244). Cancer Res 2010;70:2264–73.
10. Loboda A, Nebozhyn M, Klinghoffer R, Frazier J, Chastain M, Arthur W, et al. A gene expression signature of RAS pathway dependence predicts response to PI3K and RAS pathway inhibitors and expands the population of RAS pathway activated tumors. BMC Med Genet 2010;3:26. doi: 10.1186/1755-8794-3-26.
11. Lake D, Corrêa SAL, Müller J. Negative feedback regulation of the ERK1/2 MAPK pathway. Cell Mol Life Sci 2016;73:4397–413.
12. O'Hagan RC, Tozer RG, Symons M, McCormick F, Hassell JA. The activity of the Ets transcription factor PEA3 is regulated by two distinct MAPK cascades. Oncogene 1996;13:1323–33.
13. Whitmarsh AJ. Regulation of gene transcription by mitogen-activated protein kinase signaling pathways. Biochim Biophys Acta 2007;1773:1285–98.
14. Murphy LO, MacKeigan JP, Blenis J. A network of immediate early gene products propagates subtle differences in mitogen-activated protein kinase signal amplitude and duration. Mol Cell Biol 2004;24:144–53.
15. Sanjana NE, Shalem O, Zhang F. Improved vectors and genome-wide libraries for CRISPR screening. Nat Methods 2014;11:783–4.
16. Holzel M, Huang S, Koster J, Ora I, Lakeman A, Caron H, et al. NF1 is a tumor suppressor in neuroblastoma that determines retinoic acid response and disease outcome. Cell 2010;142:218–29.

17. Jing J, Greshock J, Holbrook JD, Gilmartin A, Zhang X, McNeil E, et al. Comprehensive predictive biomarker analysis for MEK Inhibitor GSK1120212. Am Assoc Cancer Res 2012;11:720–9.
18. Garnett MJ, Edelman EJ, Heidorn SJ, Greenman CD, Dastur A, Lau KW, et al. Systematic identification of genomic markers of drug sensitivity in cancer cells. Nature 2012;483:570–5.
19. Berry T, Luther W, Bhatnagar N, Jamin Y, Poon E, Sanda T, et al. The ALKF1174L mutation potentiates the oncogenic activity of MYCN in Neuroblastoma. Cancer Cell 2012;22:117–30.
20. Cazes A, Lopez-Delisle L, Tsarovina K, Pierre-Eugène C, Preter KD, Peuchmaur M, et al. Activated Alk triggers prolonged neurogenesis and Ret upregulation providing a therapeutic target in ALK-mutated neuroblastoma 2014.
21. Zhang W, Yu Y, Hertwig F, Thierry-Mieg J, Zhang W, Thierry-Mieg D, et al. Comparison of RNA-seq and microarray-based models for clinical endpoint prediction. Genome Biol 2015;16:1–12.
22. Asgharzadeh S, Pique-Regi R, Sposto R, Wang H, Yang Y, Shimada H, et al. Prognostic significance of gene expression profiles of metastatic neuroblastomas Lacking MYCN gene amplification. J Natl Cancer Inst 2006;98:1193–203.
23. Limpt Vv, Schramm A, Lakeman A, Sluis Pv, Chan A, Noesel Mv, et al. The Phox2B homeobox gene is mutated in sporadic neuroblastomas. Oncogene 2004;23:9280–8.
24. Reiff T, Tsarovina K, Majdazari A, Schmidt M, del Pino I, Rohrer H. Neuroblastoma Phox2b variants stimulate proliferation and dedifferentiation of immature sympathetic neurons. J Neurosci 2010;30:905–15.
25. Dissanayake K, Toth R, Blakey J, Olsson O, Campbell David G, Prescott Alan R, et al. ERK/p90(RSK)/14–3–3 signalling has an impact on expression of PEA3 Ets transcription factors via the transcriptional repressor capicúa. Biochem J 2011;433:515–25.
26. Iorio F, Knijnenburg Theo A, Vis Daniel J, Bignell Graham R, Menden Michael P, Schubert M, et al. A landscape of pharmacogenomic interactions in cancer. Cell 2016;166:740–54.
27. Bresler Scott C, Weiser Daniel A, Huwe Peter J, Park Jin H, Krytska K, Ryles H, et al. ALK mutations confer differential oncogenic activation and sensitivity to ALK inhibition therapy in neuroblastoma. Cancer Cell 2014;26:682–94.
28. Yaari S, Jacob-Hirsch J, Amariglio N, Haklai R, Rechavi G, Kloog Y. Disruption of Cooperation Between Ras and MycN in human neuroblastoma cells promotes growth arrest. Clin Cancer Res 2005;11:4321–30.
29. Chibon F.Cancer gene expression signatures—the rise and fall? Eur J Cancer 2013;49:2000–9.
30. Raabe EH, Laudenslager M, Winter C, Wasserman N, Cole K, LaQuaglia M, et al. Prevalence and functional consequence of PHOX2B mutations in neuroblastoma. Oncogene 2008;27:469–76.
31. Wang Y, Marino-Enriquez A, Bennett RR, Zhu M, Shen Y, Eilers G, et al. Dystrophin is a tumor suppressor in human cancers with myogenic programs. Nat Genet 2014;46:601–6.
32. Fernandez K, Serinagaoglu Y, Hammond S, Martin LT, Martin PT. Mice lacking dystrophin or α sarcoglycan spontaneously develop embryonal rhabdomyosarcoma with cancer-associated p53 mutations and alternatively spliced or mutant Mdm2 transcripts. Am J Pathol 2010;176:416–34.
33. Okimoto RA, Breitenbuecher F, Olivas VR, Wu W, Gini B, Hofree M, et al. Inactivation of Capicua drives cancer metastasis. Nat Genet 2016; advance online publication.
34. Futran AS, Kyin S, Shvartsman SY, Link AJ. Mapping the binding interface of ERK and transcriptional repressor Capicua using photocrosslinking. Proc Natl Acad Sci 2015;112:8590–5.
35. Molenaar JJ, Koster J, Zwijnenburg DA, van Sluis P, Valentijn LJ, van der Ploeg I, et al. Sequencing of neuroblastoma identifies chromothripsis and defects in neuritogenesis genes. Nature 2012;483:589–93.
36. Fransson S, Ostensson M, Djos A, Javanmardi N, Kogner P, Martinsson T. Estimation of copy number aberrations: comparison of exome sequencing data with SNP microarrays identifies homozygous deletions of 19q13.2 and CIC in neuroblastoma. Int J Oncol 2016;48:1103–16.